Article citation info:
Rymaniak Ł, Sobczak J, Szymlet N, Pielecha P, Wiśniewski S. Emission testing of diesel multiple units complying with different emission standards during real operating conditions. Rail Vehicles/Pojazdy Szynowe. 0000;xx:xx-xx. https://doi.org/10.53502/ RAIL-202044

Rail Vehicles/Pojazdy Szynowe

www.railvehicles.eu

Emission testing of diesel multiple units complying with different emission standards during real operating conditions

Łukasz **Rymaniak** [a, *], Jakub **Sobczak** [a], Natalia **Szymlet** [a], Piotr **Pielecha** [b], Sławomir **Wiśniewski** [b]

[a] *Institute of Powertrains and Aviation, Poznan University of Technology, Poznan, Poland*
[b] *Doctoral School, Poznan University of Technology, Poland*

ARTICLE INFO

Received: 10 December 2024
Revised: 18 February 2025
Accepted: 19 February 2025
Available online: 20 February 2025

KEYWORDS

exhaust emission
railbus
real operating conditions
PEMS
combustion engines

This article presents comparative studies on pollutant emissions from railbuses meeting different emission standards (Stage IIIA and Stage IIIB). Measurements were conducted under real-world operating conditions on routes regularly serviced by the tested vehicles during passenger operations. The obtained results enabled the evaluation of vehicle operating conditions and propulsion systems, the assessment of emission intensity as a function of driving parameters, the determination of road-specific and unit-specific emission factors, and comparisons with homologation limits. The vehicle compliant with the newer emission standard demonstrated a reduced environmental impact, particularly regarding particulate matter emissions. Object A achieved 0.03 g/km and 0.005 g/kWh in the test, while the second object achieved 0.14 g/km and 0.03 g/kWh. Significant differences were also recorded for CO. The object with the higher approval standard achieved a CO emission of 9 g/km and 1.36 g/kWh. For vehicle B, obtained 14.71 g/km and 3.22 g/kWh respectively. However, the analysis revealed that selected toxic compounds exceeded legislated limits during testing. The tested vehicles exceeded the permitted NO_x and HC pollutant emission standards by between 5% and 50%.

1. Introduction

Rail transport is one of the key sectors for passenger and freight mobility in Poland. In 2023, the number of passengers opting for this mode of transport exceeded 374 million, marking a record high for the 21st century [17]. It provides an excellent alternative to road transport for daily commuter connections between suburban areas and city centers. Moreover, rail transport offers the capacity to move larger volumes of goods per unit trip compared to other modes of transport.

With growing public awareness of ecology and environmental protection, rail transport aligns perfectly with the current European Union trends of decarbonizing the transport sector [20]. However, it is important to note that electric rail vehicles, despite producing no direct emissions, still exert an indirect environmental impact by transferring emissions to the locations of power plants. These power plants, under Poland's current energy structure, predominantly rely on fossil fuels. Additionally, only 63% of the railway network in Poland is electrified [2]. The remaining 7000 kilometers of rail lines continue to utilize locomotives or railcars equipped with conventional propulsion systems.

Efforts to reduce exhaust emissions aim to mitigate their adverse effects on human health and the natural environment. Regional rail routes and lines with lower passenger volumes often employ railbuses, which are an excellent alternative to conventional locomotives or railcars, enabling lower pollutant emissions levels, such as nitrogen oxides (NO_x), carbon oxides (CO_x), hydrocarbons (HC), and particulate matter (PM) and particulate number (PN) [6, 7, 19]. However, the harmfulness of emissions depends on the operating characteristics of the propulsion system and varies significantly under real-world conditions due to nu-

* Corresponding author: lukasz.rymaniak@put.poznan.pl (Ł. Rymaniak)

merous factors [10, 14]. Consequently, traditional laboratory homologation methods for exhaust emissions fail to accurately reflect the real-world conditions of units equipped with conventional propulsion systems [13, 21]. To address the real-world environmental impact, there has been an increasing use of on-road testing methods that enable a realistic evaluation and comparison of emissions against legally established norms and limits. Moreover, advancements in portable measurement technology (PEMS – Portable Emissions Measurement Systems) allow for studying the influence of factors such as passenger load, atmospheric conditions, idle operation, and full-load operation on exhaust emissions in real-world tests [1, 5, 18]. In recent years, research focused on evaluating the actual emissions from both on-road and off-road vehicles has gained significant traction [8, 11, 16].

As part of the ongoing research efforts to understand the real-world impact of internal combustion vehicles on the environment, this study was undertaken. The objective of this paper is to determine the influence of operational parameters on the intensity of harmful exhaust compounds and to evaluate their magnitude relative to the homologation standards of the tested objects. Measurements were conducted on two vehicles characterized by different emission homologation standards. The tests were performed under real-world operating conditions using a proprietary methodology and state-of-the-art measurement equipment from the PEMS category.

2. Research methodology

The first tested vehicle was a railbus operated in Poland, compliant with the Stage IIIB emission standard (vehicle A, Fig. 1). This vehicle is equipped with two compression-ignition (CI) engines, each delivering 390 kW of power and a maximum torque of 2300 Nm (Table 1). The second test object was a diesel multiple unit (DMU), representing an older model of railbus manufactured since 2005. It meets the Stage IIIA emission standard (vehicle B, Fig. 2). Its propulsion system consists of two drive units, each equipped with a CI engine producing 350 kW of power and a maximum torque of 1700 Nm. For passenger safety, both vehicles underwent technical inspections before testing to rule out any defects that might have directly influenced the final results of the toxic compound emissions tests. Both rail vehicles share similar operational parameters, including comparable passenger capacities and the same maximum operating speed of 120 km/h. In the analytical part of this study, the vehicles are referred to as research object A and research object B, respectively.

Fig. 1. Diesel multiple unit – research object A

Fig. 2. Diesel multiple unit – research object B

Table 1. Characteristic of diesel powertrains of research objects

Parameter	Vehicle A	Vehicle B
Propulsion type	2 × CI engine	
Power [kW]	390	350
Torque [Nm]	2300	1700
Exhaust emission standard	Stage IIIB	Stage IIIA
Exhaust aftertreatment systems	DOC+DPF+SCR	DOC

The measurement equipment used in the study, part of the PEMS group, was the Axion R/S+ system (Fig. 3). Manufactured by the American company Global MRV, this device has been validated by the Environmental Technology Verification (ETV) program, conducted by the United States Environmental Protection Agency (USEPA). The analyzers integrated into the device enable the measurement of harmful emissions from exhaust systems, including CO, CO_2, HC, NO_x, PM, and O_2. Concentrations of CO, CO_2, and HC are measured using an NDIR (Nondispersive Infrared Sensor) analyzer. PM emissions are measured using the Laser Scatter method, while NO_x and O_2 levels are determined with electrochemical analyzers, which generate an electrical signal. The device's specifications are outlined in Table 2. The apparatus is also equipped with a GPS (Global Positioning System) module for positioning. Data measurements are carried out at a frequency of 1 Hz. To obtain a comprehensive analytical dataset, including parameters

such as engine speed, torque, pressures, and temperatures, a TEXA Navigator TXTs TRUCK diagnostic tester with data recording capability was employed. The exhaust gas flow is calculated based on data from the on-board diagnostic system.

Fig. 3 Research equipment – Axion R/S+ [3]

Table 2. Characteristic of Axion R/S+ [3]

Gas	Range	Accuracy	Resolution	Measurement method
HC	0–2000 ppm	±4 ppm	1 ppm	NDIR
CO	0–10%	±0.02%	0.001%	NDIR
CO_2	0–16%	±0.3%	0.01%	NDIR
NO	0–5000 ppm	±5 ppm	1 ppm	Electrochemical
O_2	0–25%	±0.02%	0.01%	Electrochemical
PM	0–50 mg/m^3	±2%	0.01 mg/m^3	Laser Scatter

The vehicles were tested on different routes, designated according to the vehicles: Route A (Fig. 4) and Route B (Fig. 5).

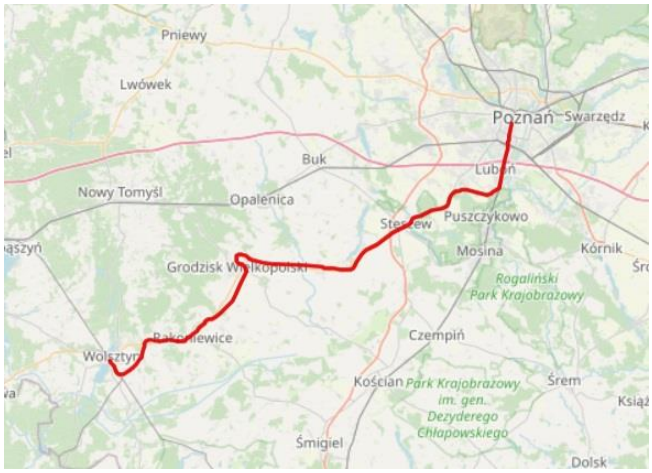

Fig. 4. Test route A for research object A: Poznan–Wolsztyn [4]

The measurement conditions were aligned with the operational usage of the test objects, as these routes are regularly serviced by the selected vehicles. The length of Route A, serviced by the first test object, was 79.63 km, while the second test object covered 56.95 km during testing. The operational characteristics of the railbuses on their respective routes are detailed in Table 3.

Table 3. Characteristic of research routes

Parameter	Route A	Route B
Route length [km]	79.63	56.95
Travel time [s]	5303	3807
Average velocity [km/h]	54.02	53.85
Number of stops	19	18
Total time stop [s]	655	398

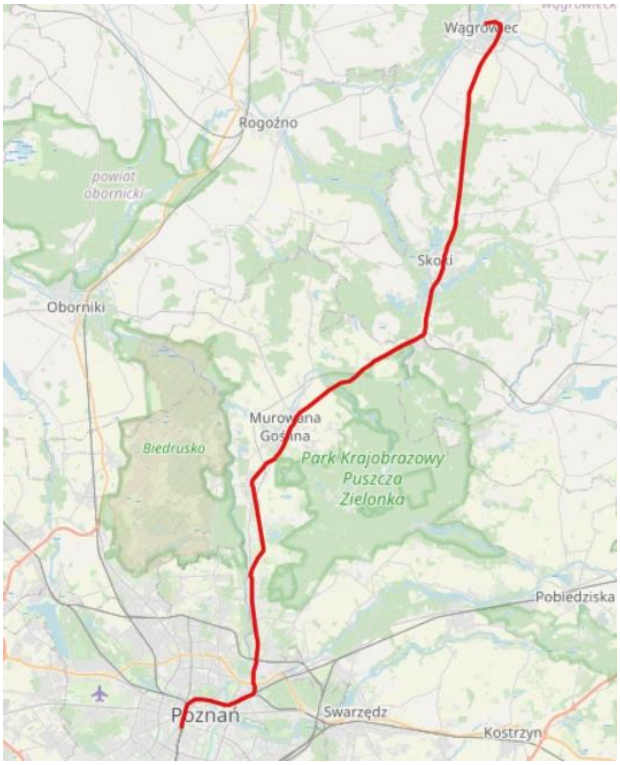

Fig. 5. Research route B for research object B: Poznan–Wagrowiec [4]

3. Analysis of motion parameters

Based on the data recorded by the GPS system, the speed profiles of the test objects during the experimental runs were determined (Fig. 6). The average speed for both routes differed by only 0.19 km/h. The average speed of research object A was 54.02 km/h, while that of research object B was 53.85 km/h. In both cases, the rail vehicles spent the majority of the time either accelerating or decelerating. Research object A predominantly operated at speeds below 100 km/h due to the limitations of the railway infrastructure. In contrast, research object B exceeded 100 km/h for approximately 360 seconds, particularly during the initial phase of the test.

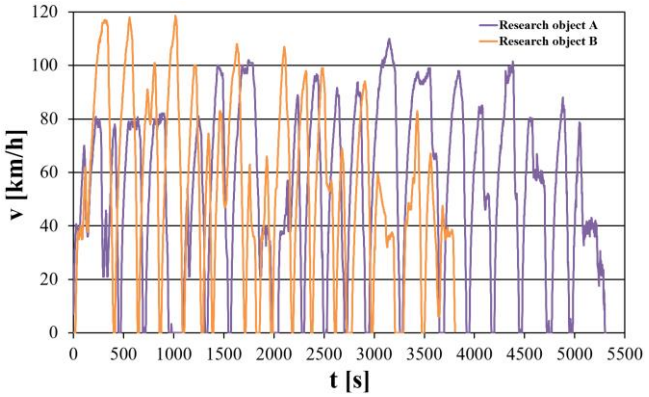

Fig. 6. Speed profiles of the research objects

The measurement data obtained under real-world operating conditions, covering vehicle speed and acceleration ranges as well as engine operating parameters, were correlated with their respective temporal shares during the tests. A discrete mathematical model based on a probability function – time density – was employed for this purpose. Figure 7 illustrates the operational time distribution for research object A. The highest share, 12.35% of the total measurement time, was recorded during idling. The cumulative operational time share in the acceleration range (0 m/s²; 0.7 m/s²⟩ amounted to 39.03%. A share of 17.6% was recorded for steady-speed operation. Dynamic accelerations and decelerations contributed marginally to the total time, primarily due to the mass and inertia of the test object. The cumulative operational time for decelerations in the range (…; –0.7 m/s²⟩ was 4.71%, while for accelerations in the range (0.7 m/s²; …) it was 1.98%. For research object B the highest individual operational time share was recorded in the vehicle speed range (40 km/h; 60 km/h⟩, accounting for 21.6%. The time share for deceleration in the range (–0.7 m/s²; 0 m/s²⟩ was 25.6%, while idling accounted for a total time share of 10.45%.

To perform a comprehensive analysis of operational parameters, time-density characteristics were determined for the research objects as a function of engine operating parameters. For research object A, the engine operating parameters were most frequently observed in three ranges (Fig. 8). Within the torque range (…; 400 Nm⟩ and rotational speed ranges (800 rpm; 1000 rpm⟩ and (1000 rpm; 1200 rpm⟩, the recorded operational time accounted for 29.96% and 13.75% of the total runtime, respectively. During vehicle acceleration, the engine predominantly operated within the rotational speed ranges (1600 rpm; 1800 rpm⟩ and (2000 Nm; …), with a time share of 25.14%. For research object B, the recorded time distribution was more balanced. Within the low-load torque range to 400 Nm, the engine operated across a wide range of rotational speeds, with a cumulative time share of 42.6%. During transit under increasing speed conditions, the engine primarily operated within the torque range (800 Nm; 2000 Nm⟩ and rotational speed range (1400 rpm; 1600 rpm⟩. The cumulative time share for this crankshaft speed range was 26.2%.

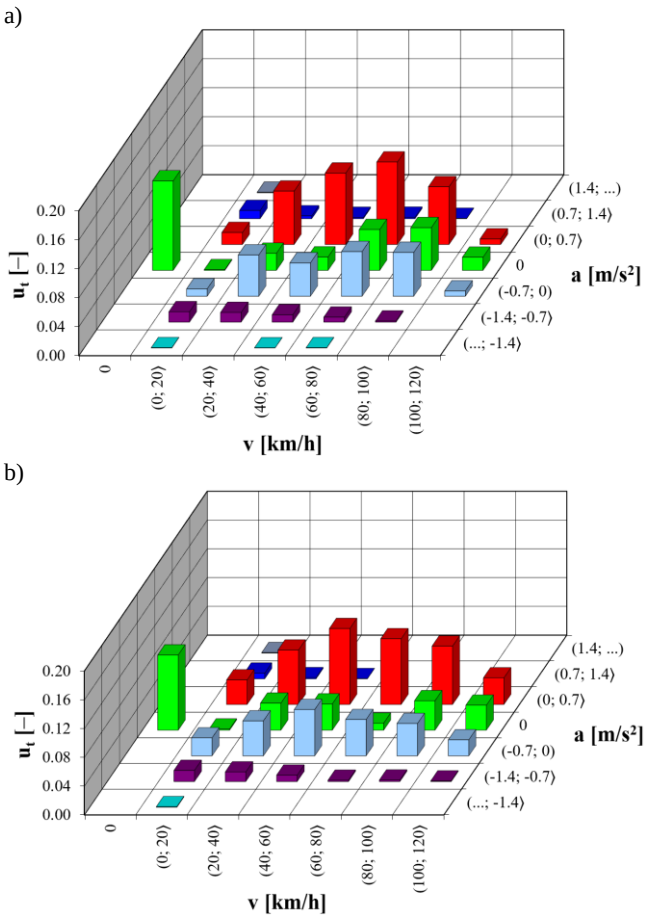

Fig. 7. Operating time shares in speed and acceleration ranges for research object: a) A on route A, b) B on route B

The performance of the research objects in real-world operation is similar in terms of movement parameters, especially in the parking range. However, the driveline performance parameters are different. This is due to differences in the design of the powertrains presented. The mechanical work generated by the internal combustion engine in test facility A is transferred to a traction generator, where the energy is converted into electrical energy. The current is then transferred to the main rectifier. It then goes to the traction inverter, which is also connected to the braking resistors. The current then goes to the asynchronous traction motors, which convert the electrical energy into mechanical energy that is transferred to the vehicle's drive bogies. The propulsion system of research object B consists of two powertrain assemblies. Each unit consists of an internal combustion engine with an integrated retarder. The power of the drive unit is transmitted via a Cardan shaft to an in-

termediate axle gearbox (with a built-in reversing gear – on the first wheel of each drive bogie).

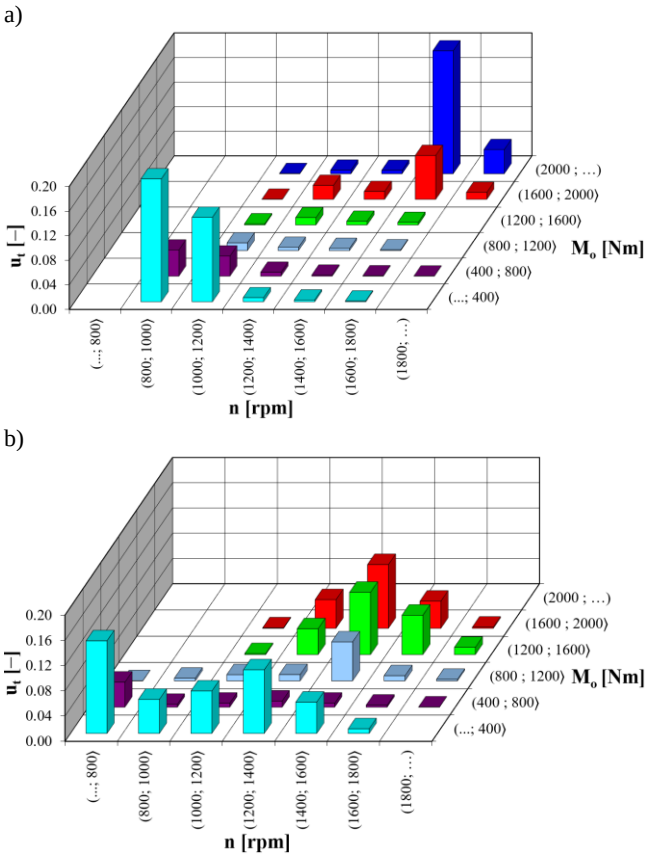

Fig. 8. Operating time shares in engine speed and torque ranges for research object: a) A on route A, b) B on route B

4. Analysis of toxic compound emissions intensity

The emission intensity values of harmful compounds were evaluated in relation to the operating conditions of rail vehicles. Emission intensities for the two test vehicles were compared using identical ranges for speeds, accelerations, torques, and crankshaft rotational speeds. For research object A, the highest carbon monoxide (CO) emission intensity (Fig. 9a) was recorded during vehicle idling, reaching 431.03 mg/s. Under steady-state operation at speeds within the range (0 km/h; 20 km/h⟩, the emission intensity was 250.73 mg/s, which may indicate suboptimal performance of the oxidation catalyst at low or zero speeds. The average CO emission intensity at speeds of (40 km/h; 60 km/h⟩ with deceleration in the range (…; –1.4 m/s²⟩ was 275.93 mg/s. Notably, abrupt braking negatively impacts carbon monoxide emissions.

For research object B (Fig. 9b), the highest average CO emission intensity was observed at speeds of (0 km/h; 20 km/h⟩ with accelerations in the range (1.4 m/s²; …), corresponding to a dynamic start of the rail vehicle. Similarly high average intensities were recorded in the speed range (0 km/h; 20 km/h⟩ for lower acceleration intervals of (0.7 m/s²; 1.4 m/s²⟩ and (0 m/s²; 0.7 m/s²⟩, yielding emission intensities of 642.8 mg/s and 492 mg/s, respectively. This highlights adverse combustion phenomena during vehicle acceleration. However, such issues are less pronounced in the newer vehicle, attributed to the installation of an oxidation reactor capable of converting toxic carbon monoxide into less harmful compounds.

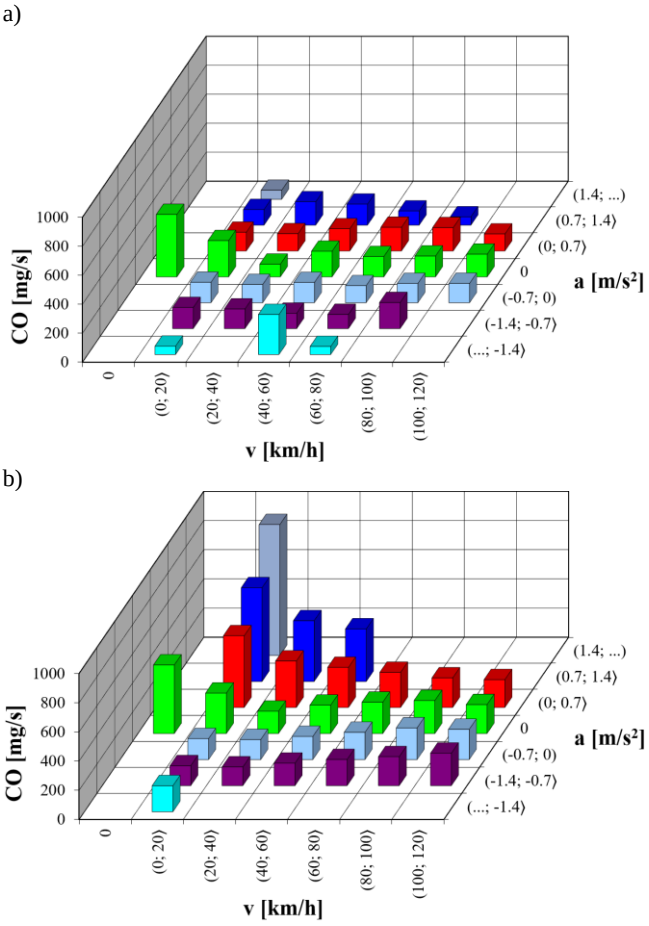

Fig. 9. CO emission intensity in speed and acceleration ranges: a) for research objects A, b) for objects B

The distribution of average HC emission intensity for research object A (Fig. 10a) closely mirrors that of the average carbon monoxide (CO) emission intensity, with only minor differences of approximately 0.2% across the respective intervals. This similarity arises from the comparable mechanisms underlying the formation of these toxic compounds. Moreover, the use of a combined oxidation reactor for CO and HC contributed to a uniform reduction in their concentrations. For research object B (Fig. 10b), the highest HC emission intensity was recorded during vehicle idling.

Significant HC emission intensity was also observed in the acceleration range (0.7 m/s²; 1.4 m/s²⟩ at speeds within the intervals (40 km/h; 60 km/h⟩ and (60 km/h; 80 km/h⟩. This indicates unfavorable combustion conditions during rapid vehicle acceleration, which is further evident in the range (1.4 m/s²; …),

where the emission intensity reached 43.7 mg/s. The average emission intensities for lower acceleration and deceleration conditions were found to be at a comparable level.

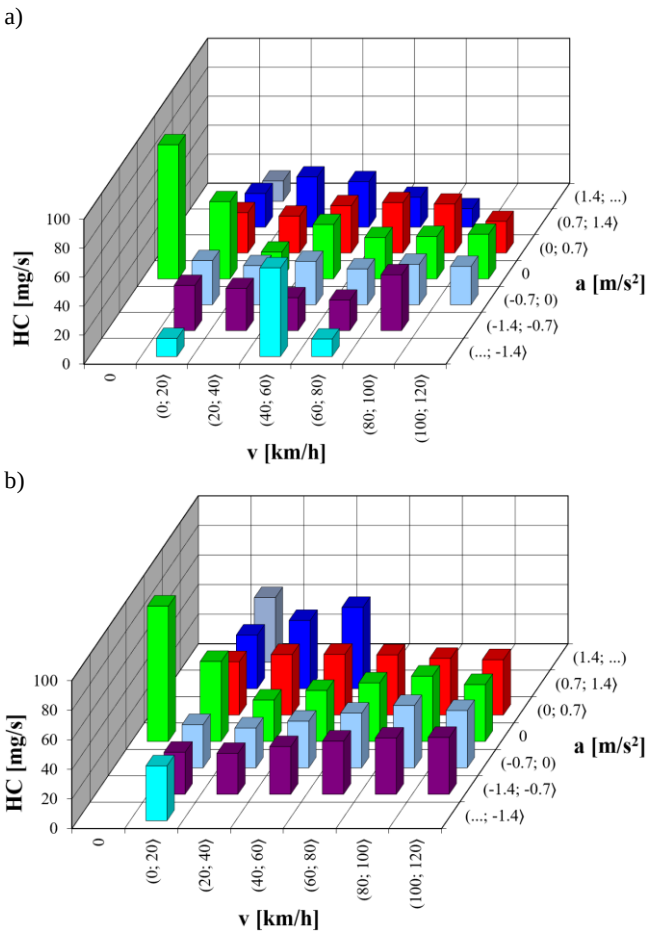

Fig. 10. HC emission intensity in speed and acceleration ranges: a) for research objects A, b) for object B

The results of NO_x emissions for research object A are presented in Fig. 11. The highest emission intensity, 551.3 mg/s, was recorded during accelerations in the range (0.7 m/s²; 1.4 m/s²⟩ at vehicle speeds between (20 km/h; 40 km/h⟩. Overall, the emission intensities during acceleration were cumulatively higher than those recorded during deceleration intervals. The primary factor driving NO_x formation is the elevated temperatures and pressures in the combustion chamber, which are more pronounced during vehicle acceleration due to the rapid increase in engine load.

For research object B (Fig. 11b), increased NO_x emission intensity was similarly observed during vehicle acceleration, attributable to the combustion chamber conditions. The highest NO_x emission intensities were recorded during idling and steady-speed operation within the speed range (0 km/h; 20 km/h⟩, reaching 1002.98 mg/s and 754.24 mg/s, respectively. Compared to the emission intensities of the newer vehicle, these values were nearly twice as high. One of the key factors contributing to the reduction of NO_x emissions in the newer vehicle was the more advanced exhaust gas recirculation (EGR) system. However, the most significant impact on the results was attributed to the selective catalytic reduction (SCR) system, which is responsible for the targeted catalytic reduction of nitrogen oxides.

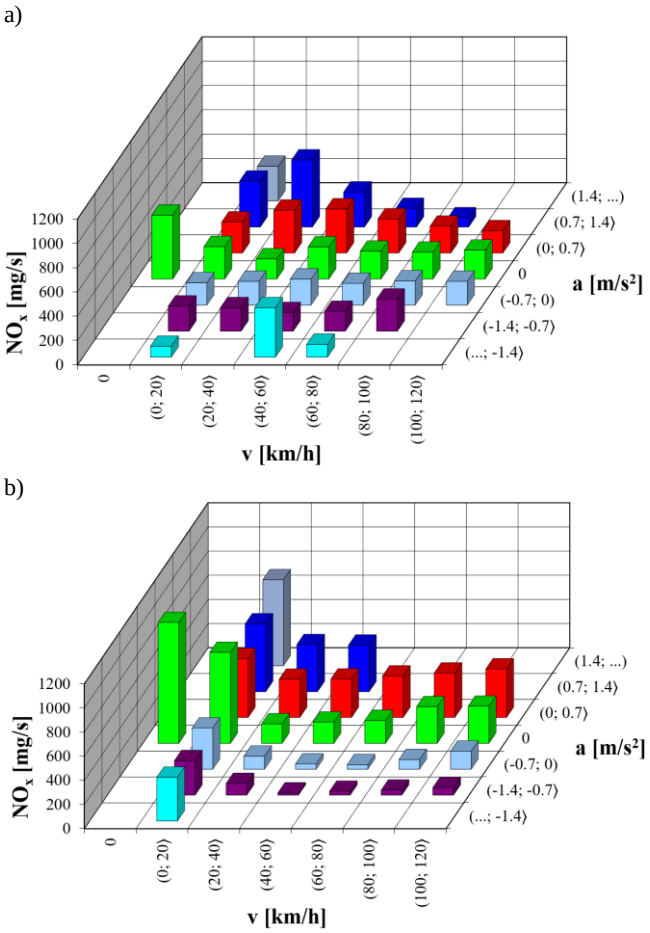

Fig. 11. NO_x emission intensity in speed and acceleration ranges: a) for research object A, b) for object B

The highest PM emission intensities for research object B (Fig. 12b) were recorded during vehicle acceleration within the speed range (0 km/h; 20 km/h⟩. This was particularly pronounced for dynamic accelerations in the range (1.4 m/s²; …), where the PM emission intensity reached 27.6 mg/s. This result is attributed to the increased engine workload during vehicle startup from a station, associated with high load conditions. Under these circumstances, incomplete and inefficient combustion occurs, promoting the formation of soot and, consequently, particulate matter. In contrast, for the vehicle equipped with a Diesel Particulate Filter (DPF) (Fig. 12a), the PM emission intensity distribution was more uniform. The highest values were observed during vehicle idling – 1.77 mg/s and during rapid acceleration (1.4 m/s²; …) at speeds within the range (0 km/h; 20 km/h⟩, where

the intensity reached 1.4 mg/s. This highlights the effectiveness of the DPF in mitigating particulate emissions even under high-load and dynamic conditions.

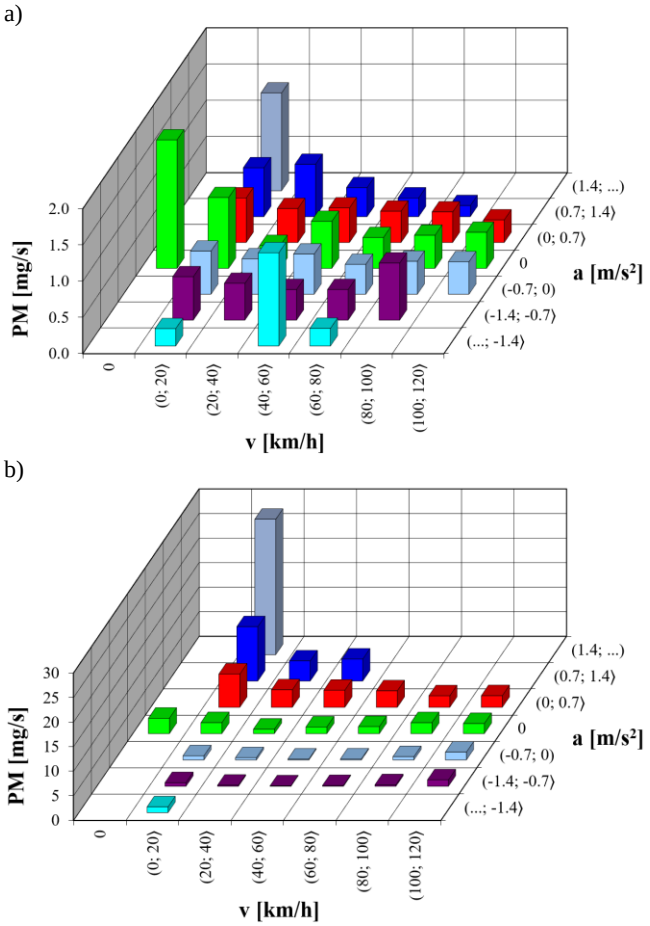

Fig. 12. PM emission intensity in speed and acceleration ranges: a) for research object A, b) for object B

5. Comparison of road and specific emissions for the research objects

For rail vehicles complying with Stage emission standards, pollutant emissions are typically expressed in specific terms (g/kWh). However, due to the operational nature of the tested objects, the authors proposed a comparative evaluation in terms of road emissions. Based on measurements conducted under real-world operating conditions, both specific emissions and road emissions of harmful compounds from the exhaust systems of the diesel multiple units were determined. The analysis compared object B, which complies with the Stage IIIA emission standard, with object A, which complies with the Stage IIIB standard. Figure 13 illustrates the comparison of road emissions of pollutants. The most significant difference between the tested vehicles is observed in CO emissions. For object A, the road emission was 9 g/km, whereas for object B, it was 14.71 g/km. The primary source of this substantial difference lies in the more advanced exhaust after-treatment systems. The newer vehicle complying with the Stage IIIB standard is equipped with a DOC system, which oxidizes CO and HC. Hydrocarbons emissions are also reduced by 0.5 g/km due to the installation of the DOC system. Road emissions of PM for the older vehicle were 4.5 times higher than for object A. This is because vehicles meeting Stage IIIB and later standards are equipped with DPF to meet PM emission requirements.

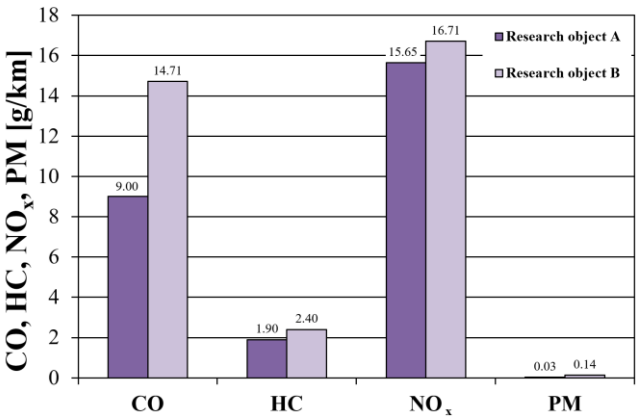

Fig. 13. Road emission of toxic compounds for research objects

Analyzing the obtained results of specific emissions of toxic compounds from exhaust systems (Fig. 14), the positive impact of implementing additional exhaust after-treatment systems between the newer and older rail vehicles can be assessed. For object A, the CO emission was 1.36 g/kWh, which is nearly 2.5 times lower than that of object B. The HC emission in this comparison is nearly two times lower, highlighting the beneficial effects of the oxidation reactor in the newer vehicle. Thanks to the installation of a DPF in object A, the specific emission of PM was lower. Furthermore, this vehicle emitted 2.36 g/kWh of NO_x, whereas its older counterpart emitted 3.66 g/kWh.

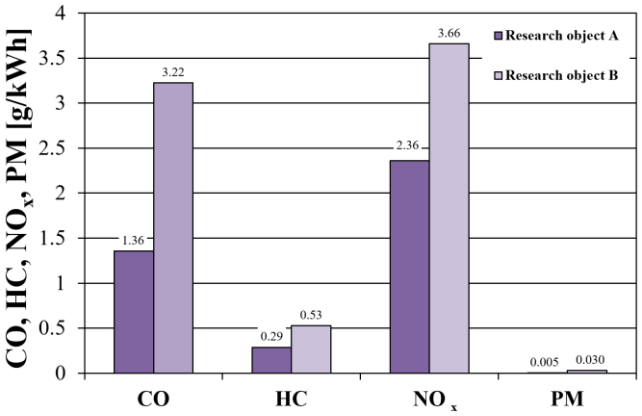

Fig. 14. Specific emission of toxic compounds for research objects

The specific emission results of harmful compounds obtained from tests conducted under real operating conditions can be compared to homologation requirements for internal combustion engines as defined by emission standards. For comparison purposes, it is necessary to calculate the emission factor k_j, as was done in studies such as [11]. The first research object complies with the Stage IIIB emission standard, while the second research object meets the Stage IIIA standard. Due to differences in the homologation methods for engines subject to the older standard, a combined emission factor for HC and NO_x was determined. In the Stage IIIB standard, these two compounds are treated separately; therefore, for hydrocarbons and nitrogen oxides in the case of test object A, two separate factors were calculated. Additionally, the obtained values for CO and PM were analyzed. The emission factor is defined as the ratio:

$$k_j = \frac{e_{rzecz,j}}{e_{dop,j}} \quad (1)$$

where: j – toxic compound for which the emission factor was determined, $e_{rzecz,j}$ – specific emission measured during real operating conditions [g/kWh], $e_{dop,\ j}$ – permissible specific emission according to standards [g/kWh].

The unit emission factors for CO and PM (Fig. 15) were calculated according to Eq. (1). The permissible CO value under both Stage IIIA and Stage IIIB standards remained unchanged at 3.5 g/kWh. The k_{CO} coefficients for both tested vehicles are less than 1, indicating compliance with the emission limits established by the standards. Despite the unchanged guidelines regarding unit carbon monoxide emissions, the newer rail vehicle performed better than the older one, with a k_{CO} coefficient of 0.39. Similarly to k_{CO}, the k_{PM} coefficient is significantly below the permissible value. Both vehicles achieved comparable results, differing by only 0.04 g/kWh. However, considering that the k_{PM} coefficient for the research object B was determined based on the permissible particulate matter limit for the Stage IIIA standard, which is eight times higher than that for object A, it can be concluded that the implementation of additional exhaust aftertreatment systems, such as a particulate filter, had a positive impact when comparing different generations of vehicles.

For the research object A, compliant with the Stage IIIB standard, separate emission limits apply for NO_x and HC. In contrast, for research object B, a combined emission factor was determined for NO_x and HC. The k_{HC} coefficient was calculated at 1.51, indicating an exceedance of the permissible HC limit. While the DOC reactor installed in the vehicle effectively oxidized CO, this came at the expense of exceeding the allowable hydrocarbon levels. In the case of the k_{NOx} coefficient, its value was 1.18, which also indicates a breach of the permissible limit established by the standards. The combined emission factor k_{HC+NOx} for research object B was 1.05, representing a slight exceedance of the permissible threshold for this vehicle.

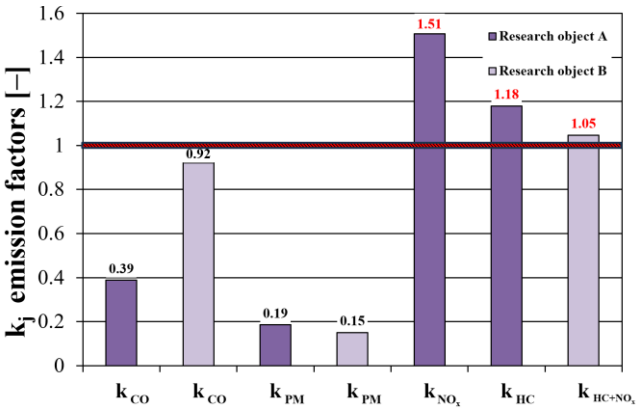

Fig. 15. The emission factor k_j for: CO, PM, NO_x and HC

6. Conclusions

Rail buses are increasingly becoming a viable alternative to road vehicles in passenger transportation, particularly in servicing areas near large urban agglomerations. Research into their environmental impact is essential not only for the design and optimization of their propulsion systems but also for organizational activities such as traffic planning, station construction, and infrastructure development. Understanding operational conditions is also crucial in developing innovative propulsion technologies or vehicle components, such as hydrogen-fueled engines, fuel cells, or advanced braking systems [9, 12, 15].

This paper examines the influence of operational parameters on the emission intensity of harmful exhaust compounds and evaluates their magnitude concerning homologation standards of the tested vehicles. Measurements were conducted on two vehicles with distinct emission homologation levels under real operating conditions, on routes they regularly service. The operating parameters of the two research objects were similar, especially in the parking range. However, the performance of the powertrains was different due to the use of different propulsion systems. Vehicle A was characterised by a traditional system, where diesel-electric propulsion was used (traction motors in the bogies). The second vehicle used a mechanical solution with a retarder. Mechanical work was transferred from the internal combustion engines via a Cardan shaft to the transmission. This had a direct impact on the higher proportion of drive time in the load range up to 400 Nm. This was achieved for the

vehicles in this range for object A at around 30% and object B at 43%, respectively.

Rail buses are homologated as non-road vehicles and their emissions are determined in g/kWh. However, given their intended use, the authors also assessed road emissions. The analyses demonstrated that the vehicle meeting the newer emission standard had a significantly lower environmental impact, particularly concerning PM emissions. Object A achieved 0.03 g/km and 0.005 g/kWh in the test, while the second object achieved 0.14 g/km and 0.03 g/kWh. Significant differences were also recorded for CO. The object with the higher approval standard achieved a CO road emission of 9 g/km and 1.36 g/kWh. For vehicle B, obtained 14.71 g/km and 3.22 g/kWh respectively. Significant differences were also shown for NO_x, in terms of specific emissions, where objects A and B achieved 2.36 g/kWh and 3.66 g/kWh respectively.

However, the study revealed that selected toxic compounds in the tests exceeded legislative limits. An emission factor was determined for comparison with the emission limits. Its application proved that CO and PM emissions did not exceed the standards. Exceedances ($k > 1$) were obtained for HC and NO_x in the value range 1.05–1.51. It should be noted that the emissions individually (for object A) and as a sum (for object B) were compared in accordance with the legislative guidelines. The comparison of emissions was carried out with reference to dynamic type-approval tests.

Future research will focus on vehicles equipped with more advanced propulsion systems. The evaluation of particulate matter emissions will be expanded to include dimensional and numerical distributions. Additionally, emission indicators will be determined concerning passenger-kilometer metrics.

Acknowledgements

The study presented in this article was performed within statutory research (No. 0415/SBAD/0351).

Nomenclature

CI	compression ignition
CO	carbon monoxide
CO_2	carbon dioxide
DOC	diesel oxidation catalyst
DMU	diesel multiple unit
DPF	diesel particulate filter
EGR	exhaust gas recirculation
HC	hydrocarbons
NDIR	nondispersive infrared sensor
NO_x	nitrogen oxides
PEMS	portable emission measurement system
PM	particulate matter
PN	particulate number
SCR	selective catalytic reduction

Bibliography

[1] Bodisco T, Zare A. Practicalities and driving dynamics of a real driving emissions (RDE) Euro 6 regulation homologation test. Energies. 2019;12(12):2306. https://doi.org/10.3390/en12122306

[2] Dmitrowicz-Życka K. Przewozy ładunków i pasażerów w 2023 r. Główny Urząd Statystyczny (in Polish); 2024 May. https://stat.gov.pl/obszary-tematyczne/transport-i-lacznosc/transport/przewozy-ladunkow-i-pasazerow-w-2023-roku,11,12.html (accessed on 2024.12.03).

[3] GlobalMRV. Axion R/S+ PEMS. https://www.globalmrv.com/products/axion-rs-2-pems/ (accessed on 2024.12.05).

[4] GPS Visualizer. https://www.gpsvisualizer.com/ (accessed on 2024.12.08).

[5] Huang C, Lou D, Hu Z, Feng Q, Chen Y, Chen C et al. A PEMS study of the emissions of gaseous pollutants and ultrafine particles from gasoline- and diesel-fueled vehicles. Atmos Environ. 2013;77:703-710. https://doi.org/10.1016/j.atmosenv.2013.05.059

[6] Kirschstein T, Meisel F. GHG-emission models for assessing the eco-friendliness of road and rail freight transports. Transportation Res B-Meth. 2015;73:13-33. https://doi.org/10.1016/j.trb.2014.12.004

[7] Landwehr KR, Larcombe AN, Reid A, Mullins BJ. Critical review of diesel exhaust exposure health impact research relevant to occupational settings: are we controlling the wrong pollutants? Expos Health. 2021; 13:141-171. https://doi.org/10.1007/s12403-020-00379-0

[8] Merkisz J, Gallas D, Siedlecki M, Szymlet N, Sokolnicka B. Exhaust emissions of an LPG powered vehicle in real operating conditions. E3S Web of Conferences. https://doi.org/10.1051/e3sconf/201910000053

[9] Pielecha I, Szwajca F. Cooperation of a PEM fuel cell and a NiMH battery at various states of its charge in a FCHEV drive. Eksploat Niezawodn. 2021;23(3):468-475. https://doi.org/10.17531/ein.2020.1.15

[10] Pielecha J, Skobiej K. Evaluation of ecological extremes of vehicles in road emission tests. Archives of Transport. 2020;56(4):33-46. https://doi.org/10.5604/01.3001.0014.5516

[11] Rymaniak Ł, Wiśniewski S, Woźniak K, Frankowski M. Evaluation of pollutant emissions from a railbus in real operating conditions during transport work. Combustion Engines. 2023;194(3):84-88. https://doi.org/10.19206/CE-169138

[12] Sawczuk W, Jüngst M, Kaczmarek D. Model of energy consumption by brake discs of rail vehicles. Rail Vehicles/Pojazdy Szynowe. 2024;1-2:11-20. https://doi.org/10.53502/RAIL-186984

[13] Siedlecki M, Szymlet N, Sokolnicka B. Influence of the particulate filter use in the spark ignition engine vehicle on the exhaust emission in real driving emission test. Journal of Ecological Engineering. 2020; 21(1):120-127. https://doi.org/10.12911/22998993/113073

[14] Skobiej K, Pielecha J. Analysis of the exhaust emissions of hybrid vehicles for the current and future RDE driving cycle. Energies. 2022;15(22). https://doi.org/10.3390/en15228691

[15] Szwajca F, Gawrysiak C, Pielecha I. Effects of passive pre-chamber jet ignition on knock combustion at hydrogen engine. Combustion Engines. 2024;198(3): 110-122. https://doi.org/10.19206/CE-189738

[16] Szymlet N, Kamińska M, Ziółkowski A, Sobczak J. Analysis of non-road mobile machinery homologation standards in relation to actual exhaust emissions. Energies. 2024;17(15):3624. https://doi.org/10.3390/en17153624

[17] Urząd Transportu Kolejowego. Sektor Kolejowy (in Polish). 2023. https://www.sektorkolejowy.pl/utk-sprawozdanie-z-funkcjonowania-rynku-transportu-kolejowego-w-2023-r/ (accessed on 2024.12.03).

[18] Vlachos TG, Bonnel P, Perujo A, Weiss M, Villafuerte PM, Riccobono F. In-use emissions testing with portable emissions measurement systems (PEMS) in the current and future European vehicle emissions legislation: overview, underlying principles and expected benefits. Commercial Vehicles. 2014;7(1):199-215. https://doi.org/10.4271/2014-01-1549

[19] Vojtisek-Lom M, Jirků J, Pechout M. Real-world exhaust emissions of diesel locomotives and motorized railcars during scheduled passenger train runs on Czech railroads. Atmosphere. 2020;11(6):582. https://doi.org/10.3390/atmos11060582.

[20] Winnett J, Hoffrichter A, Iraklis A, McGordon A, Hughes DJ, Ridler T et al. Development of a very light rail vehicle. P I Civil Eng-Transp. 2017;170(4): 231-342. https://doi.org/10.1680/jtran.16.00038

[21] Ziółkowski A, Fuć P, Lijewski P, Rymaniak Ł, Daszkiewidcz P, Kamińska M et al. Analysis of exhaust emission measurements in rural conditions from heavy-duty vehicle. Combustion Engines. 2020; 182(3):54-58. https://doi.org/10.19206/CE-2020-309